Photothermal deflection study of V/V_2O_5 alternating layers structure: effect of annealing atmospheres on thermal and optical properties

Anouar Khalfaoui[a,*] **Soufiene Ilahi**[a,b] **and Noureddine Yacoubi**[a]
[a]Université de Carthage, IPEIN, Laboratoire: Physique, Mathématiques, Modélisation Quantique et Conception Mécanique LR-18E S45, Nabeul, Tunisie
[b]Université de Monastir, Faculté des Sciences de Monastir, Département de Physique, Monastir, Tunisie

Abstract. High sensitivity uncooled microbolometers are necessary to meet the needs of the next generation of infrared detectors, and vanadium oxide thin films are the potential candidates for uncooled microbolometers due to their high temperature coefficient of resistance (TCR) at room temperature. It is, however, very difficult to deposit vanadium oxide thin films having a high temperature coefficient of resistance because of the process limits in microbolometer fabrication. We present a fabrication method for vanadium oxide thin films. Through the formation of a vanadium oxide V_xO_y thermometer thin films with thickness of 95 nm prepared by sputter-depositing nine alternative layers of V_2O_5 and V of thicknesses of 15 and 5 nm, respectively. Two samples of vanadium oxide mixed phase are characterized in this work and compared to a not annealed sample, the first sample is annealed at 300°C for 30 min in O_2 and the second in N_2 atmosphere. The results show that annealing atmosphere has an effect on microstructure, optical, and thermal properties of the mixed phase. Comparing to our previous work, we have reached in this work successful results with vanadium oxide sample having both high TCR and low resistivity. [DOI: 10.1117/1.JRS.16.014521]

Keywords: microbolometer; vanadium oxide; sandwich structure; photothermal deflection technique.

Paper 210354 received Jun. 3, 2021; accepted for publication Feb. 25, 2022; published online Mar. 17, 2022.

1 Introduction

Until now, the development of IR imaging systems has been of growing interest due to the wide range of application from military, civilian night vision, mine detection, surveillance, and medical imaging.[1–4] The recent advances in micromachining technology have made it possible to fabricate highly sensitive thermal IR microbolometer detection that can be operated at room temperature.[5]

V_xO_y thin film is one of the most commercially sensitive materials for microbolometer,[6–19] which is counted as a smart material. Besides the most popular thin films of vanadium oxide, other materials have been studied as thermal-sensitive element for bolometer, such as metal films,[20] yttrium barium copper oxide (Yba Cuo),[21–23] polycrystalline silicon germanium (SiGe),[24] and amorphous silicon (α-Si).[18,25]

The amorphous silicon can be used as a unique sandwich structure which consists of the segregation layer located between the metal and the active layers. It requires high annealing temperature of about 1000°C to achieve stability of microstructure. The temperature coefficient of resistance (TCR) value of A-Si microbolometer is about −2.8%/K. It was suggested that the A-Si bolometer has higher temperature sensitivity and a detectivity that depends strongly on frequency.[25]

*Address all correspondence to Anouar Khalfaoui, anouar_khalfaoui@yahoo.fr

At room temperature, material temperature coefficient of resistance (TCR) is an important factor for infrared sensors performance,[26–28] and the bolometer with high TCR has reached detectivity of $(1.0 \times 10^9\ \text{cm}\,\text{Hz}^{1/2}/\text{W})$.[28]

Due to the strong effect of deposition parameters on the composition and microstructure of vanadium oxides, different phases can be obtained by changing the deposition process parameters. They undergo transition from an insulator or semiconductor to a metal phase at a specific temperature.

In our previous works, we have determined electrical, thermal, and optical properties of different multilayer of vanadium oxide mixed phase.[9,29,30] Achieving a desirable structure with higher TCR and lower resistivity is the main motivation for using different layer structures. The target total thickness of the structure was between 80 and 120 nm, which is suitable for standard bolometer thickness. It seems that, as the number of layers is increased, the TCR increases while the resistivity decreases. The aim of using a different number of layers is to increase the percentage of V in the structure to obtain different oxides during annealing.[31] The nine alternate layers of V_2O_5/V deposited on silicon substrate have proven successful in realizing higher TCR and lower resistivity than the five alternate layers of V_2O_5/V deposited on quartz substrate.[31] We have also proposed the layer structure of the air-bridge microbolometer which presented the fabrication and design of vanadium oxide microbolometer.[32]

However, to improve the efficiency of such device, in this work, we report on the microstructural, optical, and thermal properties of the nine alternative layers of V_2O_5/V by Raman spectroscopy and photothermal deflection techniques (PDS and PDT). The results prove that changing the annealing atmospheres cause a change in Raman spectra which presents the formation of multiple phases such as VO_2, V_2O_5, and V_6O_{13}. This latter introduces a variation in the most sensitive parameters to the temperature coefficient of resistance, such as optical absorption spectra, optical band gap, and thermal conductivity.

2 Experiment

The layer structure proposed for the air-bridge microbolometer based upon the fabrication and design of vanadium oxide microbolometer is represented in Fig. 1.

The thin film thermometer material with a 95-nm-thick multilayer structure composed of nine alternating layers of V_2O_5 and V with thickness of 15 and 5 nm, respectively, was deposited at room temperature and further annealed at 300°C for 30 min in N_2 and O_2 atmospheres. As shown in Fig. 2 shows a two-dimensional schematic of the multilayer thin-film structure.

The V_2O_5 layers were deposited using RF sputtering at chamber base pressure of 2×10^{-6} Torr at 3 mTorr of Ar pressure and 150 W of RF power using 99.5% pure V_2O_5 target. The V layers were deposited using DC sputtering at chamber base pressure of 2×10^{-6} Torr at 3 mTorr of Ar pressure and 150 W of DC power using 99.8% pure V target. Deposited structures were then annealed in a tube furnace at 300°C for 30 min. The annealing was performed at O_2 and N_2 at flow rates of 120 ml/min.

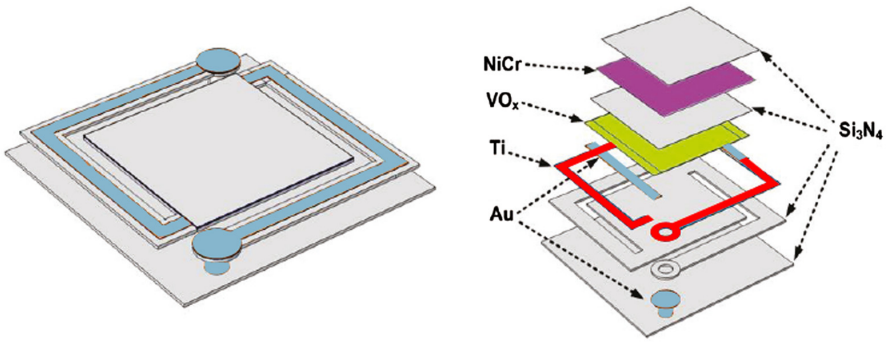

Fig. 1 The layer structure of the proposed air-bridge microbolometer.

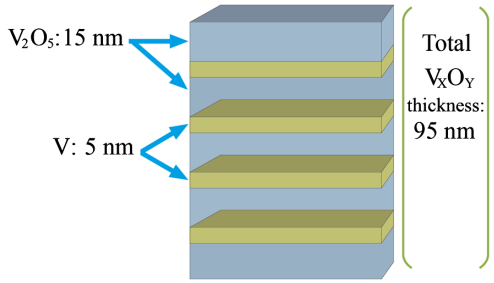

Fig. 2 Schematic diagram of the multilayer structure.

3 Results and Discussion

3.1 *Raman Spectroscopy*

Raman spectroscopy is also used, which is a sensitive tool for further investigation of the structure of a material.[33,34]

Figure 3 shows the room temperature Raman spectra using 632.8 nm excitation, of the vanadium oxide films deposited in different annealing atmosphere. The set is composed of three samples, the first annealed in O_2, annealed in N_2 and the third is not annealed for comparison.

The spectra were recorded in the range of 200 to 1200 cm^{-1}. The spectra show a broad band centered at 528 cm^{-1} which refers to the short-range order in the multiple layer sample. The appearance of the other peaks from the samples annealed in O_2 and N_2 atmosphere caused by the convolution with a vibration mode from the vanadium oxide.

The samples spectra annealed in O_2 and N_2 are dominated by emerging peaks at 169, 229, 310, 403, 528, 706, and 988 cm^{-1}.

These results suggested the formation of multiple phases of vanadium oxide. The high frequency vibration at 1000 cm^{-1} can be attributed to the terminal oxygen (VO) stretching. The vibration at about 625 and 762 cm^{-1} corresponds to the stretching vibration of V_3O.

The spectra of annealed sample in O_2 atmosphere show more peaks than the sample annealed in N_2 atmosphere and the as grown sample.

This is due to the kinetic reaction of vanadium with oxygen. The peak at 528 cm^{-1} appears in Raman spectra of all the samples which indicate the presence of V_2O_5. The peak at 310 cm^{-1} shown in the spectra of the as-grown sample and the sample annealed in N_2 atmosphere indicates the presence of VO_2. This peak disappears for an annealing in O_2 atmosphere and the presence of VO_2 is indicated in the peak at 229 cm^{-1}. We acknowledge the presence of V_6O_{13} in all Raman

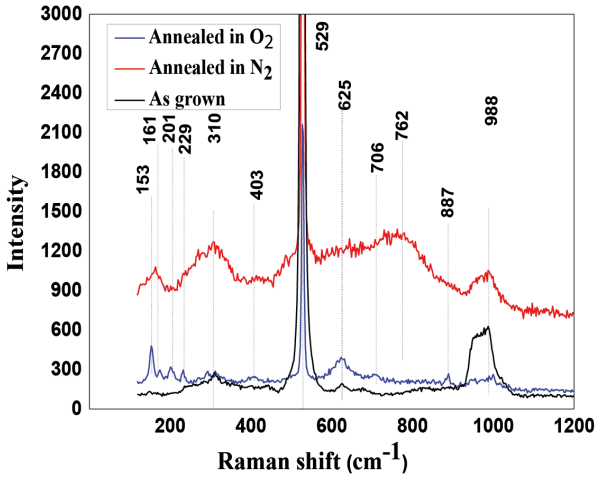

Fig. 3 Room temperature Raman spectra of the as-grown sample and samples subjected to different annealing time at 300°C for 30 min.

spectra at 988 cm^{-1}, however for the sample annealed in O_2 spectra the peaks corresponded to V_6O_{13} appears at 167 and 887 cm^{-1}.

These results are in good agreement with those obtained previously.[30]

3.2 *Photothermal Deflection Measurements*

The photothermal deflection technique PDT or "mirage effect" technique was first introduced in the early 1980s by Bocarra, Fournier, Baldoz[35] and subsequently developed by Aamodt,[36] Murphy,[37] and by Jackson et al.[38] The biggest advantage of this noncontactless, nondestructive, and highly sensitive technique is the great precision for optical and thermal properties materials evaluation.[39–41]

The principle of the photothermal deflection technique or "mirage effect" consists of heating the sample (placed in a gas or liquid) with a modulated light. This heating will generate a temperature gradient therefore a refractive index gradient in the fluid in contact with the heated sample's surface, which will cause the deflection of a laser probe beam skimming the sample surface (Fig. 4).

This deflection Ψ[42] is a function of thermal and optical properties of the sample and also of the thermal properties of fluid and substrate:

$$\psi = \frac{dz}{dx} = -\frac{l}{n}\frac{dn}{dT_f}\frac{dT_f}{dz}, \tag{1}$$

where T_f is the distribution temperature elevation in the fluid and n is its refractive index.

This temperature, in the case of uniform heating, can be written

$$T_f = T_0 e^{-\sigma_f z} e^{j\omega t},$$

where T_0 is the periodic temperature elevation at the sample surface

$$\sigma_f = (1+j)\sqrt{\frac{\pi F}{D_f}},$$

where F and D_f are the modulation frequency and thermal diffusivity of the fluid, respectively.

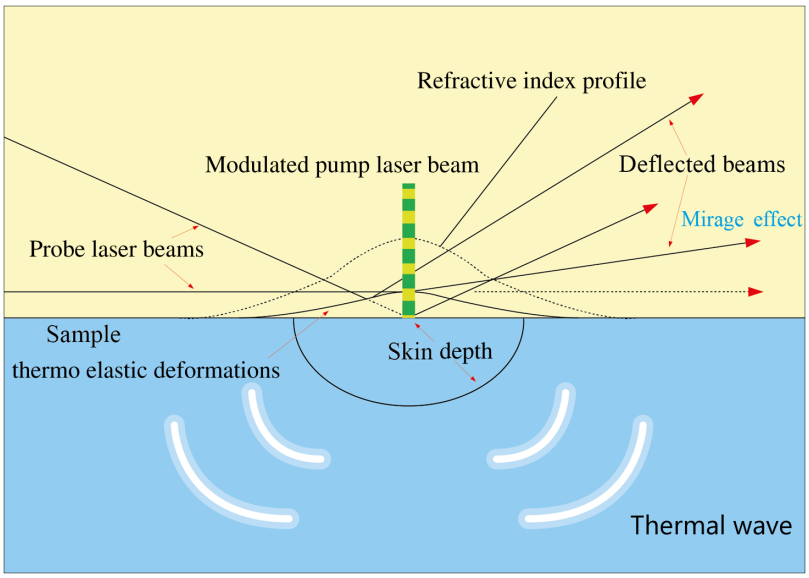

Fig. 4 Principle of photothermal deflection.

3.2.1 *Experimental setup of photothermal deflection techniques PDS and PDT*

The photothermal deflection spectroscopy mounting aims to study the variations of the photothermal signal as a function of wavelength. The experimental setup is practically the same that of Fig. 5 of PDT technique except that a monochromator was interposed between the lamp and the chopper.

PDS is a pump-probe technique. Pump and probe beams are aligned perpendicular to each other. The sample is immersed in a liquid, such as paraffin oil which exhibits a pronounced temperature dependence of its refractive index. The sample is heated by a monochromatic light coming from a halogen lamp and a monochromator and then modulated by a mechanical chopper at a constant frequency. The absorption by the sample of the modulated pump beam will generate a thermal wave that creates a refractive index gradient in the fluid. A focused laser probe beam (He–Ne laser) crossing the liquid close to the sample surface is deflected. The deflection of the probe beam is measured due to a silicon photodetector of four quadrants (QD50T) linked to a lock-in amplifier (EG&G Model 5209) giving the amplitude and the phase of the photothermal signal. A personal computer was used to store the amplitude and the phase of the signal and draw their variations with the wavelength. However, for PDT, we study the variation of amplitude and phase as a function of square root of modulation frequency. The sample in this case is placed in air. The experimental PDT setup is described in detail elsewhere.[43]

3.2.2 *Absorption spectrum*

To investigate the gap energy with great precision and determining the absorption spectrum of V_xO_y samples, we have used the highly sensitive technique PDS.

On the same sample, we have conducted a spectroscopic study. On Fig. 6(a), the experimental normalized amplitude variation with wavelength is reported. We note that the amplitude presents two saturated areas corresponding to high and very low absorption coefficients. To deduce the optical absorption spectrum of vanadium oxide multilayer thin films, we have to compare the experimental curves to the corresponding theoretical ones as shown in Fig. 6(b).

In Fig. 7 the optical absorption spectrum of the V_xO_y samples is reported.

3.2.3 *Determination of the gap energies*

Gap energy is obtained from the optical absorption spectrum using the Tauc law for energies above the gap $(\alpha E)^n = \beta(E - E_g)$ where β is a constant, E_g is the gap energy, $E = h\upsilon$ is photon

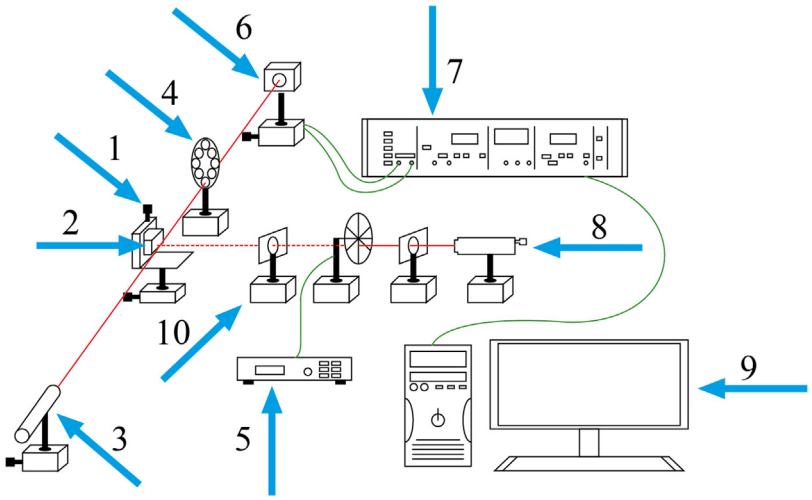

Fig. 5 Experimental set-up of PDT Technique. 1: micrometric table; 2: sample; 3: laser probe; 4: attenuator; 5: mechanical chopper; 6: four-quadrant position photodetector; 7: synchronous detection; 8: halogen lamp; 9: microcomputer.

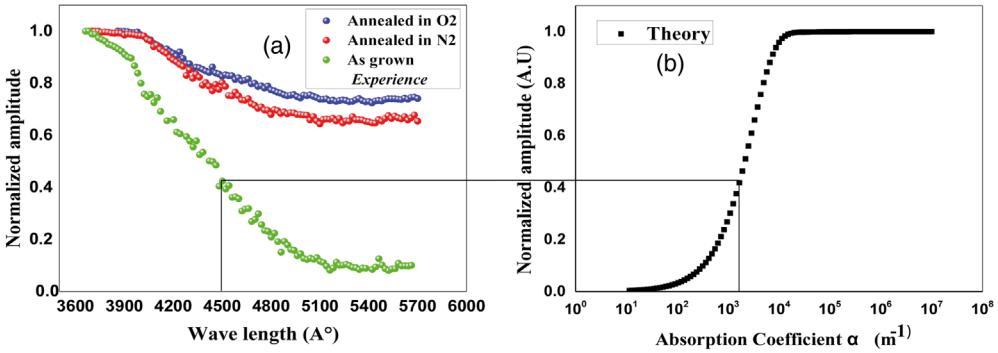

Fig. 6 Experimental (a) and theoretical (b) amplitude of PDS signals versus wavelength and absorption coefficient, respectively, of two samples of V_xO_y annealed at 300°C for 30 min in N_2 and O_2 atmosphere and not annealed sample.

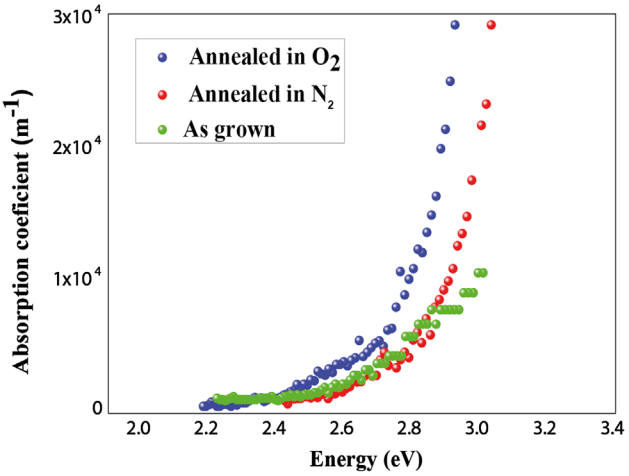

Fig. 7 Optical absorption spectra versus photon energy E of V_xO_y thin films.

energy, $n = 2$ for semiconductors having direct gap, and $n = 1/2$ for those having indirect gap. In our case, we take $n = 3/2$ for direct forbidden transition.

The variations of $(\alpha E)^n$ according to the energy E are shown in Fig. 8.

The extrapolation of the linear part of the curve intersects the axis of the energy ($\alpha = 0$) by a value corresponding to the gap energy. The calculated values are 2.49, 2.58, and 2.7 eV for as

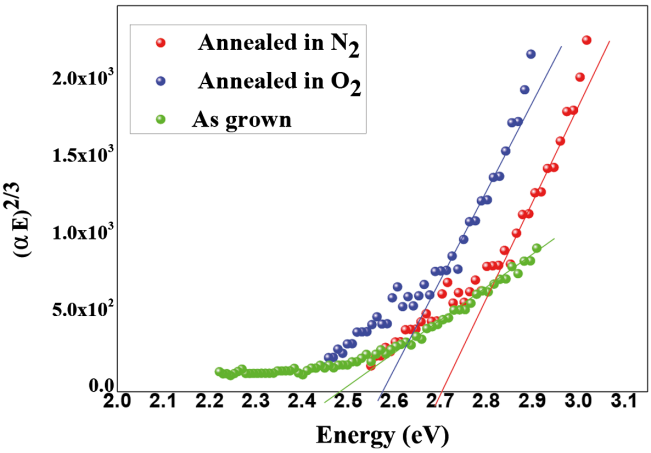

Fig. 8 $(\alpha E)^{2/3}$ versus energy E near the band gap energy.

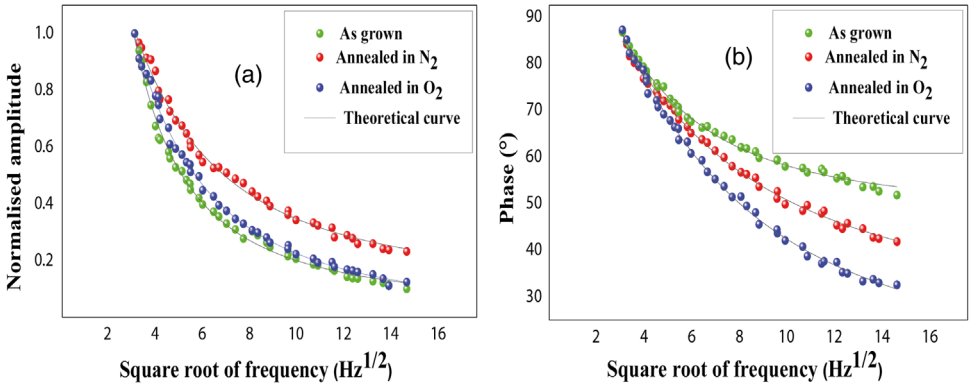

Fig. 9 Experimental (points) and theoretical (line) photothermal signals versus modulation frequency for V_xO_y samples annealed at 300°C for 30 min in various annealing atmospheres.

grown and annealed samples in O_2 and N_2 atmosphere, respectively. Obtained results are comparable with the values reported by several authors.[44–46]

3.2.4 *Thermal properties*

Thermal conductivity measurements for the synthesized V_xO_y thin films were investigated by PTD technique. Theoretical simulation consists of fitting the experimental amplitude and phase with theoretical ones obtained by the complex expression of the deflection function given by Ref. 42. The curves of Fig. 9 represent the experimental and theoretical variations of the amplitude and the phase of the photothermal signal according to the square root of frequency. The best fit of the signal amplitude and the phase variation yields an estimation of the thermal conductivity of the layered V_xO_y film.

The calculated values of thermal conductivity are 1.96 ± 0.01, 2.55 ± 0.02, and 3.6 ± 0.02 $W.m^{-1}.K^{-1}$ for as grown and for annealed samples in O_2 and N_2 atmospheres, respectively. Thus, the best TCR value is found to be $-3.06\%/K$ and the lower resistivity equal to 0.84 Ω.cm for the sample annealed in O_2 atmosphere; however, for the sample annealed in N_2 atmosphere has demonstrated high TCR $-3.55\%/K$ and high resistivity 2.68 Ω.cm.[31]

The increase of thermal conductivity for V_xO_y annealed in N_2 atmosphere refers to two main reasons, the first reason relies on the reduced defects density and especially oxygen-related vacancies annihilation by thermally activated atomic diffusion and/or intermixing. The second reason can be linked to the microstructural properties of the V_xO_y films.[29,30] The observed behavior is confirmed by Raman spectroscopy as shown in Fig. 2. It suggests different phases of V_xO_y to be formed at different annealing atmosphere.

The obtained results are in good agreement with values reported in our previous work.[9,29] However, in the present work, we have reached successful results using the nine alternating layers of V/V_2O_5 deposited on silicon and annealed at 300°C for 30 min in O_2 atmosphere.

4 Conclusion

High TCR and low resistivity are the most needed parameters for vanadium oxide thin films integrated for microbolometer applications. These latter could be achieved by growing mixed phase of V and V_2O_5. Mixed phase vanadium oxide films were grown by sputter deposition in oxygen and nitrogen atmosphere at 300°C for 30 min. This study proves that changing the atmosphere of deposition will beget a changing in microstructure and so a variation in optical and thermal properties. Annealing in N_2 atmosphere increases thermal conductivity and the gap energy. We have realized remarkable results with 95 nm V_xO_y thin films annealed in O_2 atmosphere, and we obtain both high TCR and low resistivity and a suitable optical and thermal properties for microbolometer application.

References

1. J. Yu et al., "Facile color tuning method of VO_2 thin film for smart window applications," *Sci. Adv. Mater.* **8**, 2153–2157 (2016).
2. K. Schneider, M. Lubecka, and A. Czapla, "VOX thin films for gas sensor applications," *Procedia Eng.* **120**, 1153–1157 (2015).
3. Y. Gao et al., "Nanoceramic VO_2 thermochromic smart glass: a review on progress in solution processing," *Nano Energy* **1**, 221–246 (2012).
4. D. C. Bock et al., "Batteries used to power implantable biomedical devices," *Electrochim. Acta* **84**, 155–164 (2012).
5. S. V. Grayli et al., "Room temperature deposition of highly sensitive vanadium oxide films for infrared light sensing applications," in *IEEE Sens. Conf.*, Busan, Korea (2015).
6. E. M. Smith et al., "Dual band sensitivity enhancements of a VOx microbolometer array using a patterned gold black absorber," *Appl. Opt.* **55**, 2071–2078 (2016).
7. Y. O. Jin et al., "Potential for reactive pulsed-dc magnetron sputtering of nanocomposite VOx microbolometer thin films," *J. Vac. Sci. Technol. A* **32**(5), 061501 (2014).
8. C. Lamsal and N. M. Ravindra, "Simulation of spectral emissivity of vanadium oxides (VOx)-based microbolometer structures," *Emerg. Mater. Res.* **3**, 194–202 (2014).
9. B. Wang et al., "Nanostructured vanadium oxide thin film with high TCR at room temperature for microbolometer," *Infrared Phys. Technol.* **57**, 8–13 (2013).
10. M. E. Smith et al., "Dual band sensitivity enhancements of a VOx microbolometer array using a patterned gold black absorber," *Appl. Opt.* **55**(8), 2071–2078 (2016).
11. Y. H. Han et al., "Enhanced characteristics of an uncooled microbolometer using vanadium-tungsten oxide as a thermometric material," *Appl. Phys. Lett.* **86**, 254101 (2005).
12. Y. H Han et al., "Properties of electrical conductivity of amorphous tungsten-doped vanadium oxide for uncooled microbolometers," *Solid State Phenom.* **124–126**, 343–346 (2007).
13. R. T. Rajendrakumar et al., "Study of a pulsed laser deposited vanadium oxide based microbolometer array," *Smart Mater. Struct.* **12**(2), 188–192 (2003).
14. H. Wang, X. Yi, and S. Chen, "Low temperature fabrication of vanadium oxide films for uncooled bolometric detectors," *Infrared Phys. Technol.* **47**, 273–277 (2006).
15. S. C. Chen et al., "Vanadium oxide thin films deposited on silicon dioxide buffer layers by magnetron sputtering," *Thin Solid Films* **497**, 267–269 (2006).
16. Y. H. Han et al., "Fabrication and characterization of bolometric oxide thin film based on vanadium–tungsten alloy," *Sens. Actuator A Phys.* **660**, 123–124 (2005).
17. Y. H. Han et al., "Fabrication of vanadium oxide thin film with high-temperature coefficient of resistance using $V_2O_5/V/V_2O_5$ multi-layers for uncooled microbolometers," *Thin Solid Films* **425**, 260–264 (2003).
18. V. G. Malyarov, I. A Khrebtov, and Y. V. Kulikov, "Comparative investigations of the bolometric properties of thin film structures based on vanadium dioxide and amorphous hydrated silicon," *Proc. SPIE* **3819**, 136–142 (1999).
19. V. Zerov et al., "Vanadium oxide films with improved characteristics for ir microbolometric matrices," *Tech. Phys. Lett.* **27**, 378–380 (2001).
20. K. C. Liddiard, "Thin-film resistance bolometer IR detectors," *Infrared Phys.* **24**, 57–64, 1984.
21. A. Jahanab, C. M. Travers, and Z. Celik-Butler, "A semiconductor YBaCuO microbolometer for room temperature IR imaging," *IEEE Trans. Electron Devices* **44**, 1795–1801 (1997).
22. V. S. Jagtap, A. F. Dégardin, and A. J. Kreisler, "Low temperature amorphous growth of semiconducting Y–Ba–Cu–O oxide thin films in view of infrared bolometric detection," *Thin Solid Films* **520**(14), 4754–4757 (2012).
23. M. Danerud et al., "Nonequilibrium and bolometric photoresponse in patterned YBa2Cu3O7−δ thin films," *J. Appl. Phys.* **76**, 1902 (1994).
24. V. Leonov et al., "Micromachined poly-SiGe bolometer arrays for infrared imaging and spectroscopy," *Proc. SPIE* **4945**, 54–63 (2002).
25. X. M. Liu, L. Han, and L.T. Liu, "A novel uncooled a-Si microbolometer for infrared detection," in *8th Int. Conf. Solid-State and Integrated Circuit Technol. Proc.*, IEEE (2006).

26. C. Chen et al., "Linear uncooled microbolometer array based on VOx thin films," *Infrared Phys. Technol.* **42**(2), 87–90 (2001).
27. R. H. Chen, Y. L. Jiang, and B. Z. Li, "Influence of post-annealing on resistivity of VOx thin film," *IEEE Electron Device Lett.* **35**, 780–782 (2014).
28. A. Khalfaoui et al., "Photothermal deflection technique investigation of annealing temperature and time effects on optical and thermal conductivity of V/V_2O_5 alternating layers structure," *Physica B* **522**, 26–30 (2017).
29. M. Abdel-Rahman et al., "Temperature coefficient of resistance and thermal conductivity of vanadium oxide 'Big Mac' sandwich structure," *Infrared Phys. Technol.* **71**, 127–130 (2015).
30. B. Ilahi et al., "Thermal annealing induced multiple phase in V/V_2O_5 alternating multilayer structure," *Int. J. Mod. Phys. B* **30**(27), 1650210 (2016).
31. M. F. Zia et al., "Electrical and infrared optical properties of vanadium oxide semiconducting thin-film thermometers," *J. Electron. Mater.* **46**(10), 5978–5985 (2017).
32. M. Abdel-Rahman et al., "Fabrication and design of vanadium oxide microbolometer," *AIP Conf. Proc.* **1809**, 020001 (2017).
33. X. J. Wang et al., "XRD and Raman study of vanadium oxide thin films deposited on fused silica substrates by RF magnetron sputtering," *Appl. Surf. Sci.* **177**, 8–14 (2001).
34. C. Zhang, "Characterization of vanadium oxide thin films with different stoichiometry using Raman spectroscopy," *Thin Solid Films* **620**, 64–69 (2016).
35. A.C. Boccara, D. Fournier, and J. Baldoz, "Thermo-optical spectroscopy: detection by the "mirage effect," *Appl. Phys. Lett.* **36**, 130 (1980).
36. L. C. Aamodt and J. C. Murphy, "Photothermal measurements using a localized excitation source," *J. Appl. Phys.* **52**, 4903 (1981).
37. J. C. Murphy and L. C. Aamodt, "Photothermal spectroscopy using optical beam pro-bing: mirage effect," *J. Appl. Phys.* **51**, 4580 (1980).
38. W. B. Jackson et al., "Photothermal deflection spectroscopy and detection," *Appl. Opt.* **20**, 1333–1344 (2013).
39. S. Ilahi, N. Yacoubi, and F. Genty, "Thermal annealing effects on AlGaAsSb/GaSb laser structure: bandgap energy blueshift and thermal conductivity enhancement," *Opt. Mater.* **69**, 226–229 (2017).
40. N. Yacoubi and C. Alibert, "Determination of very thin semiconductor layer thickness by a photothermal method," *J. Appl. Phys.* **69**, 8310 (1991).
41. N. Yacoubi, A. Hafaiedh, and A. Joullie, "Determination of the optical and thermal properties of semiconductors with the photothermal method," *Appl. Opt.* **33**, 7171–7174 (1994).
42. N. Yacoubi and M. Fathallah, "Spectroscopic determination of thermal diffusivity of semiconductors by photothermal deflection spectroscopy," *Proceeding of the 5th International Topical Meeting on Photoacoustic and Photothermal Phenomena*, Springer's Series in Optical Sciences, Vol. **58**, p. 341–343, Springer, Heidelberg (1987).
43. Y. Vijayakumar et al., "Influence of the substrate temperature on the structural, optical and thermoelectric properties of sprayed V_2O_5 thin films," *Mater. Technol.* **49**(3), 371–376 (2015).
44. R. M. Oksuzoglu et al., "Influence of post-annealing on electrical, structural and optical properties of vanadium oxide thin films," *Opt. Laser Technol.* **48**, 102–109 (2013).
45. G. A. Khan and C. A. Hogarth, "Optical absorption spectra of evaporated V_2O_5 and co-evaporated V_2O_5/B_2O_3 thin films," *J. Mater. Sci.* **26**(2), 412–416 (1991).
46. S. Krishnakumar and C. S. Menon, "Optical and electrical properties of vanadium pentoxide thin films," *Phys. Stat. Solidi A* **153**(2), 439–444 (1996).

Anouar Khalfaoui currently works at the Department of Physics, IPEIN. She does research in photothermal characterization of semiconductors materials, i.e., investigation of optical and thermal properties by means of PTD and PDS techniques. Her current project is thin films of V_xO_y for microbolometer application.

Soufiene Ilahi is currently working at the Department of Physics, Monastir University. He does research in photothermal characterization of semiconductors materials, i.e., investigation

of optical, thermal, and electronics properties by means of PTD and PDS techniques. His current projects are a tandem solar cell-based III-N-V/Si—GaSbbi/GaSb for mid-infrared VCSEL—GaInAsSb active layer for laser VCSEL thin VxOy for bolometer detectors.

Noureddine Yacoubi is a professor at IPEIN and head of the Photothermal Laboratory in Nabeul. He is specialized in optical and thermal characterization of materials by photothermal deflection techniques.